# Particle-Vibration Coupling Effect on the $\beta$ Decay of Magic Nuclei

Y. F. Niu (牛一斐),[1,2,*] Z. M. Niu (牛中明),[3,†] G. Colò,[1,4,‡] and E. Vigezzi[1,§]
[1]*INFN, Sezione di Milano, Via Celoria 16, I-20133 Milano, Italy*
[2]*Institute of Fluid Physics, China Academy of Engineering Physics, Mianyang 621900, China*
[3]*School of Physics and Material Science, Anhui University, Hefei 230601, China*
[4]*Dipartimento di Fisica, Unversità degli Studi di Milano, Via Celoria 16, I-20133 Milano, Italy*
(Received 30 October 2014; revised manuscript received 30 January 2015; published 8 April 2015)

Nuclear $\beta$ decay in magic nuclei is investigated, taking into account the coupling between particles and collective vibrations, on top of self-consistent random phase approximation calculations based on Skyrme density functionals. The low-lying Gamow-Teller strength is shifted downwards and at times becomes fragmented; as a consequence, the $\beta$-decay half-lives are reduced due to the increase of the phase space available for the decay. In some cases, this leads to a very good agreement between theoretical and experimental lifetimes: this happens, in particular, in the case of the Skyrme force SkM* that can also reproduce the line shape of the high-energy Gamow-Teller resonance as was previously shown.

DOI: 10.1103/PhysRevLett.114.142501 PACS numbers: 21.60.Jz, 23.40.-s, 26.30.-k

Weak interaction processes involving atomic nuclei have been the object of continuous interest for many decades [1]. The simplest process, that is, nuclear $\beta$ decay, is mainly determined by the allowed Gamow-Teller (GT) type of transition [2–4]. As a rule, most of the GT strength is concentrated in the high-energy GT resonance (GTR); consequently, the fraction that contributes to the $\beta$ decay, being in the energetically allowed region called the "$\beta$-decay window," is small. The distribution of the GT strength is governed both by the nuclear shell structure and by the still underconstrained spin-isospin channel of the nuclear effective interaction so that $\beta$-decay and GTR measurements can complement each other.

In nuclear astrophysics, the $\beta$-decay half-lives set the time scale of the rapid neutron capture process ($r$ process) and, hence, influence the production of heavy elements beyond iron in the Universe [5–7]. In particle physics, the superallowed Fermi $\beta$ decay of nuclei can be exploited to verify the unitarity of the Cabibbo-Kobayashi-Maskawa matrix [8,9].

Important advances in the measurement of the decay half-lives have been achieved in recent years with the development of radioactive ion-beam facilities. As for theory, many approaches have been formulated ranging from gross theory [10] to the interacting boson-fermion model [11]. *Ab initio* approaches can still be used only for light nuclei [12], whereas the nuclear shell model can only cover the nuclear chart up to intermediate values of A $\approx$40–50 and/or around magic regions if some frozen core is assumed. It performs quite well in reproducing $\beta$-decay half-lives in these cases (cf. e.g., the extensive studies in the $sd$ shell [13], in the $pf$ shell [14], and in heavy nuclei [15,16]; see also Ref. [17] and references therein).

Another approach, which can be applied throughout the whole isotope chart, is based on the random phase approximation (RPA) and on its extension to superfluid systems, namely, the quasiparticle RPA (QRPA). Many versions of QRPA have been applied for the study of $\beta$ decay, and most of them are based at least in part on phenomenological ingredients [18–21]. However, it would be desirable to reproduce the $\beta$-decay half-lives within the framework of a self-consistent model without adjustable parameters.

Actually, nuclear $\beta$ decay has also been investigated within self-consistent (Q)RPA models based either on nonrelativistic or on relativistic energy density functionals; in these approaches the $\beta$-decay half-lives are usually overestimated [22–25]. This deficiency can be to a good extent cured in the case of open-shell nuclei with the inclusion of an attractive isoscalar proton-neutron ($pn$) pairing force. However, the isoscalar $pn$ pairing has no, or little, effect on closed-shell or subshell nuclei such as $^{78}$Ni and $^{132}$Sn [22–25]. Therefore, there must exist other correlations, other than isoscalar $pn$ pairing, that are capable of reducing such half-lives. One possible candidate is an attractive tensor force, as it has been pointed out in Ref. [26]. It must be stressed that the introduction of new terms in the Hamiltonian, such as isoscalar $pn$ pairing or tensor terms, requires the tuning of one or more parameters. It is of considerable interest to check whether the inclusion of new correlations *without the fitting of new parameters* can improve the agreement of $\beta$-decay half-lives with experiment. A recent study [27] suggests that coupling of the GT states with two-phonon states, as well as the effect of the tensor force, increases the $\beta$-decay rates. However, the model used in Ref. [27] is not fully self-consistent since it adopts the Landau-Migdal approximation for the residual force; it also make a strong selection of two-phonon states. To investigate the role of correlations beyond mean field in a self-consistent model and in a larger model space, we apply

 

for the first time the RPA plus particle-vibration coupling (PVC) to the study of $\beta$ decay.

The RPA approach is restricted to configurations of one particle–one hole ($1p$-$1h$) nature. In order to reproduce the observed spreading widths, one must consider the damping caused by the coupling to more complicated states, like $2p$-$2h$ configurations [28–30]. An effective way to account for (most of) the observed spreading widths is to take into account the coupling of single-nucleon states to the collective low-lying (mainly surface) nuclear vibrations or phonons ($1p$-$1h$-1 phonon configurations) [31]. We call this model RPA plus PVC, and we note that self-consistent versions of such a model have been realized based on relativistic and nonrelativistic energy functionals. Good agreement with the experiment has been obtained in the case of line shape of the GT and spin-dipole strength distribution [32–35]. In our application of the RPA + PVC model, based on Skyrme energy density functionals [34,35], it was found that the coupling to phonons produces a downward shift of the GT excitation, accompanied by the development of broadening and/or fragmentation. In this Letter, we apply our Skyrme RPA plus PVC model to the study of $\beta$ decay. Our model is self-consistent in the sense that the same Skyrme force is used to calculate the single-particle levels and the RPA spectrum (both the GT one and those of the low-lying surface vibrations to be coupled to it), as well as the PVC vertices.

The RPA in its standard matrix form produces a set of $1^+$ eigenstates $|n\rangle$, having energies $E_n$ and strengths $B_n$, as well as the forward-going and backward-going amplitudes denoted by $X^{(n)}_{ph}$ and $Y^{(n)}_{ph}$, respectively. We then couple these RPA states with a set of doorway states consisting of a $p$-$h$ excitation coupled to a collective vibration. We have considered phonons with natural parity $J^\pi = 0^+$, $1^-$, $2^+$, $3^-$, $4^+$, $5^-$, and $6^+$ having energies smaller than 20 MeV and associated with a fraction of the total (isoscalar or isovector) strength larger than 5%.

The self-energy of the RPA state $|n\rangle$ is given by

$$\Sigma_n(E_M) = \sum_{ph,p'h'} W^{\downarrow}_{ph,p'h'}(E_M) X^{(n)}_{ph} X^{(n)}_{p'h'} + W^{\downarrow *}_{ph,p'h'}(-E_M) Y^{(n)}_{ph} Y^{(n)}_{p'h'}, \quad (1)$$

where the matrix elements $W^{\downarrow}_{ph,p'h'}(E_M)$ are spreading terms associated with the coupling of the $1p$-$1h$ configurations with the doorway states, defined in Refs. [34,35]. They are complex and energy dependent, calculated by using an averaging parameter $\eta$ that avoids divergences and represents, in an approximate way, the coupling of the doorway states to even more complicated configurations. We have found that the lifetimes converge for small values of $\eta$, which are expected to be appropriate for low-lying, discrete states. In our calculations, we have set $\eta = 0.05$ MeV. One can then calculate the GT strength distribution from the Gaussian averaging [36]

$$S(E_M) = \sum_n \frac{1}{\sigma_n \sqrt{2\pi}} e^{-[(E_M - E_n - \Delta E_n)^2/(2\sigma_n^2)]} B_n, \quad (2)$$

where $\sigma_n$ is defined as $\sigma_n = (\Gamma_n/2 + \eta)/\sqrt{2\ln 2}$, with $\Delta E_n = \mathrm{Re}\Sigma_n(E_M)$ and $\Gamma_n = -2\mathrm{Im}\Sigma_n(E_M)$.

Once the strength function has been obtained, the $\beta$-decay half-life of an even-even nucleus is calculated in the allowed GT approximation by using the expression [22,25,37]

$$T_{1/2} = \frac{D}{g_A^2 \int^{\Delta_{nH}} S(E_M) f(Z,\omega) dE_M} \quad (3)$$

with $D = 6163.4$ s and $g_A = 1$. The integration includes all final $1^+$ states having an excitation energy $E_M$, referred to the ground state of the mother nucleus, smaller than $\Delta_{nH} = 0.782$ MeV, which is the mass difference between neutron and hydrogen. If the energy is instead referred to the ground state of the daughter nucleus and is denoted by $E$, one has $E = E_M - \Delta B$, $\Delta B$ being the experimental binding energy difference $B_M - B_D$. This choice is often convenient, because the calculated energy of the final $1^+$ states can be directly compared to the experimental spectrum of the final nucleus. It may happen that the calculated energy of the lowest state lies at negative energy, that is, below the experimental value of the ground-state energy of the daughter nucleus. The upper limit of integration in Eq. (3) becomes equal to the $Q_\beta$ value ($\Delta_{nH} - \Delta B = Q_\beta$), namely, to the atomic mass difference between the mother and daughter nucleus. Equation (3) then becomes

$$T_{1/2} = \frac{D}{g_A^2 \int^{Q_\beta} S(E) f(Z,\omega) dE}. \quad (4)$$

The integrated phase volume $f(Z,\omega)$ is given by

$$f(Z,\omega) = \int_{m_e c^2}^{\omega} p_e E_e (\omega - E_e)^2 F_0(Z+1, E_e) dE_e, \quad (5)$$

where $p_e, E_e$, and $F_0(Z+1, E_e)$ denote the momentum, energy, and Fermi function of the emitted electron, respectively; $\omega$ is the energy difference between the initial and final nuclear state, connected with GT energy $E$ (or $E_M$) by $\omega = Q_\beta + m_e c^2 - E = \Delta_{np} - E_M$ where $\Delta_{np} = 1.293$ MeV is the mass difference between neutron and proton.

Figure 1 shows the results for the $\beta$-decay half-life of $^{78}$Ni, an important waiting-point nucleus in the $r$ process. As recalled in the beginning of this Letter and evident in the figure, the different Skyrme interactions are not well constrained in the spin-isospin channel and their predictions for the half-life at the RPA level can vary over more than 2 orders of magnitude. For instance, SAMi [38] predicts a rather collective GTR and does not leave much strength at low energy, resulting in a long half-life, at variance with SLy5 [39] that has weak spin-isospin terms

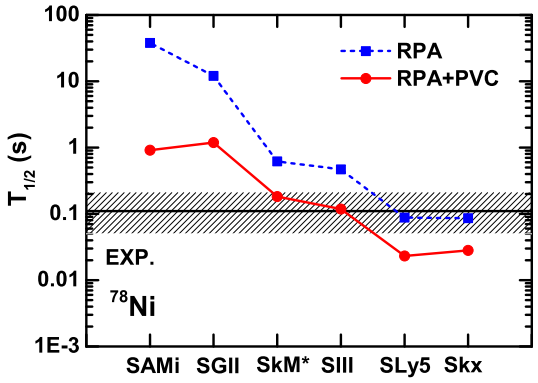


FIG. 1 (color online). $\beta$-decay half-life of $^{78}$Ni, calculated by RPA and RPA + PVC approaches with several different Skyrme interactions, in comparison with the experimental value [44].

and produces a less collective GTR, providing a much shorter half-life. The parameter sets SAMi, SGII [40], SkM* [41], and SIII [42] overestimate the half-life, while the interactions SLy5 and Skx [43] are in agreement with the experiment at the RPA level.

The inclusion of PVC effects reduces the half-lives for all interactions systematically. The reduction factor $R$ is larger for SAMi ($R \approx 42$) and SGII ($R \approx 10$) while it is equal to about 4 for the other four interactions. Within RPA + PVC, the half-life obtained with the sets SkM* and SIII falls within the experimental error. It has to be stressed that the Skyrme force SkM* not only reproduces well $\beta$-decay half-life but also the giant resonance line shape in $^{208}$Pb and $^{56}$Ni at the PVC level [34,35].

In order to understand the reasons for the systematic decrease of the half-lives after the inclusion of phonon coupling, we display in Fig. 2 the GT strength distributions (with respect to the daughter nucleus), the cumulative sums of the strengths, and the cumulative sums of $1/T_{1/2}$ [that is, the values obtained from Eq. (4) when $Q_\beta$ is replaced by a running $E$ in the upper limit of the integral in the denominator]. Generally speaking, for all nuclei under study, the GT peaks are shifted downwards when going from RPA to RPA + PVC. In $^{132}$Sn, two $1^+$ states are observed experimentally below $Q_\beta$, at $E = 1.325$ and 2.268 MeV. The latter has, however, a small decay branching ratio ($I = 0.87\%$). The lowest RPA state lies at $E = 3.6$ MeV, above the $Q_\beta$ window [Fig. 2(a)], so that the nucleus is stable. In RPA + PVC, the strength is about the same but the lowest state is shifted within the $Q_\beta$ window so that we predict a finite value of the half-life. While this is a qualitative improvement compared to RPA, the observed lowest $1^+$ state is not reproduced and the half-life is overestimated [Fig. 2(c)]. In the case of $^{68}$Ni, RPA predicts a state within the $\beta$-decay window, but its energy is higher than experiment [Fig. 2(d)] and the half-life is overestimated [the contribution of this state to $1/T_{1/2}$ is very small and is multiplied by a factor 10 in Fig. 2(f)].

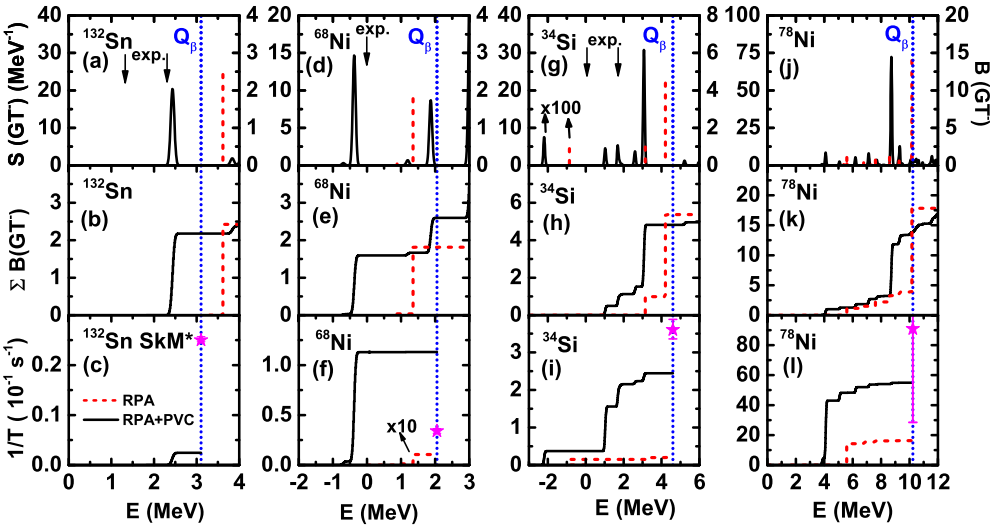


FIG. 2 (color online). Experimental data related to $\beta$ decay from nuclei $^{132}$Sn, $^{68}$Ni, $^{34}$Si, and $^{78}$Ni are compared with theoretical results obtained with the SkM* interaction. In these panels, the excitation energies $E_M$ calculated with respect to the mother nucleus are transformed to $E$, the excitation energies referred to the ground state of daughter nucleus, using experimental binding energy difference (see the text); accordingly, the vertical dotted lines show the experimental value of $Q_\beta$ [45]. Top panels: GT$^-$ low-lying strength associated with the discrete RPA peaks $B(\mathrm{GT}^-)$ (dashed lines) and with the continuous RPA + PVC strength distributions $S(\mathrm{GT}^-)$ (solid lines). The arrows indicate the experimental energies of the measured $1^+$ states [45]. Middle panels: cumulative sum of the RPA and RPA + PVC strength shown in the top panels. Bottom panels: cumulative sum of $1/T_{1/2}$. The experimental values of $1/T_{1/2}$ [45] for each nucleus are indicated by the stars. The strength of the lowest RPA and RPA + PVC peaks in panel (g) and the RPA $1/T_{1/2}$ in panel (f) have been multiplied by a factor of 100 and 10, respectively.

With the inclusion of PVC, the RPA peak at 1.5 MeV is moved even slightly below the experimental ground-state energy. This state then gives a very large contribution to $1/T_{1/2}$ because of the increased phase-space factor, although its strength is not changed much by PVC [Fig. 2(e)], and the half-life is smaller than in experiment. In the case of $^{34}$Si, in RPA one finds three peaks located at $E = -0.86$, 3.1, and 4.2 MeV. The first one lies below the experimental ground state and determines the value of $1/T_{1/2}$ [Fig. 2(i)]. This peak carries a very small value of the strength, and therefore the experimental lifetime is largely overestimated. With inclusion of the PVC, the strength becomes fragmented [Fig. 2(g)]. One can identify five peaks at $E = -2.2$, 1.0, 1.7, 2.6, and 3.1 MeV, contributing respectively 15%,49%,24%,3%, and 9% of the total value of $1/T_{1/2}$, which becomes much larger than that in RPA, substantially improving the agreement with the experimental lifetime. For the nucleus $^{78}$Ni, the small strength at $E = 5.6$ MeV gives almost all the contribution to $1/T_{1/2}$ in the RPA model [Fig. 2(l)], which underestimates the experimental value. With PVC, the state at $E = 5.6$ MeV keeps its strength but is shifted to 4.0 MeV [Fig. 2(j)] so that its contribution to $1/T_{1/2}$ becomes about 3.4 times larger [Fig. 2(l)]. The strength distribution above this peak contributes 22% of the total $1/T_{1/2}$.

The resulting calculated lifetimes for these four nuclei are compared with experiment in Fig. 3. The RPA results generally markedly overestimate the half-lives for all nuclei. An exception is represented by the interaction Skx, in which case one obtains a good agreement with data at the RPA level; this is associated with the fact that the properties of $^{132}$Sn, $^{68}$Ni, and $^{34}$Si as well as the single-particle levels of $^{132}$Sn and $^{34}$Si have been used to fit the parameters of this force [43]. The effect of the PVC decreases the values of $T_{1/2}$ by large factors compared to RPA, substantially improving the agreement with experimental data, except for Skx and (partially) for SLy5. With the inclusion of the PVC effect, the interactions SkM* and SIII give the best agreement with data. More in detail, in the case of SkM*, the lifetime is still large in $^{132}$Sn and small in $^{68}$Ni, in keeping with the errors in the position of the lowest $1^+$ state (cf. Fig. 2). Theory agrees, instead, very well with data in the case of $^{34}$Si and $^{78}$Ni.

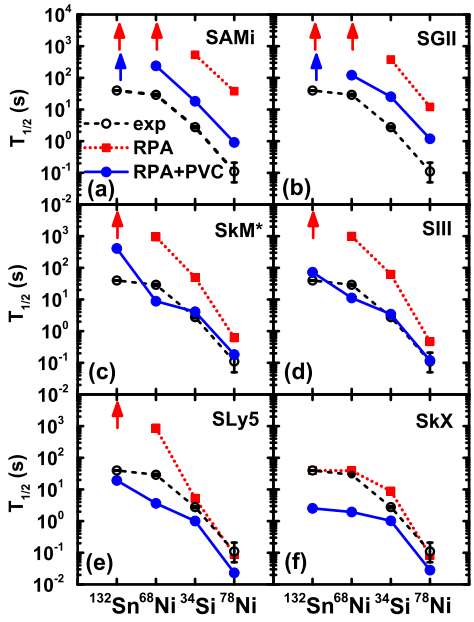


FIG. 3 (color online). The $\beta$-decay half-lives of $^{132}$Sn, $^{68}$Ni, $^{34}$Si, and $^{78}$Ni, calculated by RPA and RPA + PVC approaches, respectively, in comparison with experimental values [45]. The arrows denote half-lives longer than $10^6$ s.

In conclusion, we have shown that, starting from RPA, the coupling between particles and vibrations causes a significant downward shift in the GT strength function of these four nuclei $^{132}$Sn, $^{68}$Ni, $^{34}$Si, and $^{78}$Ni (treated as magic). The $\beta$-decay half-life is more sensitive to the position of the $1^+$ states rather than to the strength, which is not much changed in going from RPA to RPA + PVC. This is due to the strong increase of the decay phase space factor as the energy decreases. As a consequence, the lifetime is reduced in the case of RPA + PVC, and the agreement between theory and experiment is in general substantially improved. In particular, the interaction SkM* that had been previously shown to perform well in magic nuclei as far as the line shape of the GT resonance is concerned [35] leads to overall good agreement with $\beta$-decay data.

We can expect that including the effect of PVC will also be helpful in the case of other weak interaction processes, such as electron capture. PVC is expected to help with the overestimation of the threshold energy [46]. The study of open-shell nuclei by including pairing correlations is envisaged. Then the model can be employed to predict the half-lives of $r$-process bottleneck nuclei with $N = 82$, which play an important role for the duration of the $r$ process and, hence, can help to understand the origin of heavy elements in the universe.

This research was partly supported by the National Natural Science Foundation of China under Grants No. 11305161 and No. 11205004.

*nyfster@gmail.com
†zmniu@ahu.edu.cn
‡gianluca.colo@mi.infn.it
§vigezzi@mi.infn.it

[1] K. Grotz and H. Klapdor, *The Weak Interaction in Nuclear, Particle and Astrophysics* (Adam Hilger, Bristol, 1990).
[2] F. Osterfeld, Rev. Mod. Phys. **64**, 491 (1992).
[3] M. Ichimura, H. Sakai, and T. Wakasa, Prog. Part. Nucl. Phys. **56**, 446 (2006).
[4] Y. Fujita, B. Rubio, and W. Gelletly, Prog. Part. Nucl. Phys. **66**, 549 (2011).

[5] E. M. Burbidge, G. R. Burbidge, W. A. Fowler, and F. Hoyle, Rev. Mod. Phys. **29**, 547 (1957).
[6] K. Langanke and G. Martínez-Pinedo, Rev. Mod. Phys. **75**, 819 (2003).
[7] Y.-Z. Qian and G. J. Wasserburg, Phys. Rep. **442**, 237 (2007).
[8] I. S. Towner and J. C. Hardy, Rep. Prog. Phys. **73**, 046301 (2010).
[9] H. Liang, N. Van Giai, and J. Meng, Phys. Rev. C **79**, 064316 (2009).
[10] K. Takahashi, M. Yamada, and T. Kondoh, Atom. Data Nucl. Data Tables **12**, 101 (1973).
[11] F. Dellagiacoma and F. Iachello, Phys. Lett. B **218**, 399 (1989).
[12] B. R. Barrett, P. Navrátil, and J. P. Vary, Prog. Part. Nucl. Phys. **69**, 131 (2013).
[13] B. A. Brown and B. H. Wildenthal, Atom. Data Nucl. Data Tables **33**, 347 (1985).
[14] K. Langanke and G. Martínez-Pinedo, Atom. Data Nucl. Data Tables **79**, 1 (2001).
[15] G. Martínez-Pinedo and K. Langanke, Phys. Rev. Lett. **83**, 4502 (1999).
[16] T. Suzuki, T. Yoshida, T. Kajino, and T. Otsuka, Phys. Rev. C **85**, 015802 (2012).
[17] H. Li and Z. Ren, J. Phys. G **41**, 105102 (2014).
[18] I. Borzov, Nucl. Phys. **A777**, 645 (2006).
[19] D.-L. Fang, B. A. Brown, and T. Suzuki, Phys. Rev. C **88**, 034304 (2013).
[20] H. Homma, E. Bender, M. Hirsch, K. Muto, H. V. Klapdor-Kleingrothaus, and T. Oda, Phys. Rev. C **54**, 2972 (1996).
[21] P. Möller, J. R. Nix, and K. L. Kratz, Atom. Data Nucl. Data Tables **66**, 131 (1997).
[22] J. Engel, M. Bender, J. Dobaczewski, W. Nazarewicz, and R. Surman, Phys. Rev. C **60**, 014302 (1999).
[23] T. Nikšić, T. Marketin, D. Vretenar, N. Paar, and P. Ring, Phys. Rev. C **71**, 014308 (2005).
[24] T. Marketin, D. Vretenar, and P. Ring, Phys. Rev. C **75**, 024304 (2007).
[25] Z. M. Niu, Y. F. Niu, H. Z. Liang, W. H. Long, T. Nikšić, D. Vretenar, and J. Meng, Phys. Lett. B **723**, 172 (2013).
[26] F. Minato and C. L. Bai, Phys. Rev. Lett. **110**, 122501 (2013).
[27] A. P. Severyukhin, V. V. Voronov, I. N. Borzov, N. N. Arsenyev, and N. Van Giai, Phys. Rev. C **90**, 044320 (2014).
[28] V. A. Kuzmin and V. G. Soloviev, J. Phys. G **10**, 1507 (1984).
[29] S. Drożdż, S. Nishizaki, J. Speth, and J. Wambach, Phys. Rep. **197**, 1 (1990).
[30] N. D. Dang, A. Arima, T. Suzuki, and S. Yamaji, Phys. Rev. Lett. **79**, 1638 (1997).
[31] G. F. Bertsch, P. F. Bortignon, and R. A. Broglia, Rev. Mod. Phys. **55**, 287 (1983).
[32] E. Litvinova, B. A. Brown, D.-L. Fang, T. Marketin, and R. G. T. Zegers, Phys. Lett. B **730**, 307 (2014).
[33] T. Marketin, E. Litvinova, D. Vretenar, and P. Ring, Phys. Lett. B **706**, 477 (2012).
[34] Y. F. Niu, G. Colò, M. Brenna, P. F. Bortignon, and J. Meng, Phys. Rev. C **85**, 034314 (2012).
[35] Y. F. Niu, G. Colò, and E. Vigezzi, Phys. Rev. C **90**, 054328 (2014).
[36] C. Mahaux, P. F. Bortignon, R. A. Broglia, and C. H. Dasso, Phys. Rep. **120**, 1 (1985).
[37] A. de Shalit and H. Feshbach, *Theoretical Nuclear Physics: Nuclear Structure* (John Wiley and Sons, New York, 1974).
[38] X. Roca-Maza, G. Colò, and H. Sagawa, Phys. Rev. C **86**, 031306 (2012).
[39] E. Chabanat, P. Bonche, P. Haensel, J. Meyer, and R. Schaeffer, Nucl. Phys. **A635**, 231 (1998).
[40] N. Van Giai and H. Sagawa, Phys. Lett. **106B**, 379 (1981).
[41] J. Bartel, P. Quentin, M. Brack, C. Guet, and H.-B. Håkansson, Nucl. Phys. **A386**, 79 (1982).
[42] M. Beiner, H. Flocard, N. V. Giai, and P. Quentin, Nucl. Phys. **A238**, 29 (1975).
[43] B. A. Brown, Phys. Rev. C **58**, 220 (1998).
[44] P. T. Hosmer, H. Schatz, A. Aprahamian, O. Arndt, R. R. C. Clement, A. Estrade, K.-L. Kratz, S. N. Liddick, P. F. Mantica, W. F. Mueller *et al.*, Phys. Rev. Lett. **94**, 112501 (2005).
[45] http://www.nndc.bnl.gov.
[46] A. F. Fantina, E. Khan, G. Colò, N. Paar, and D. Vretenar, Phys. Rev. C **86**, 035805 (2012).